A novel CZT detector using strengthened electric field line anode*

FU Jian-Qiang(傅健强)[1,2] LI Yu-Lan(李玉兰)[1,2;1)] ZHANG Lan(张岚)[3]
NIU Li-Bo(牛莉博)[1,2] JIANG Hao(江灏)[1,2] LI Yuan-Jing(李元景)[1,2]

[1] Dept. of Engineering Physics, Tsinghua University, Beijing 100084, China
[2] Key Laboratory of Radiation Physics & Detection (Tsinghua University), Ministry of Education, Beijing 100084, China
[3] Nuctech Company Limited, Beijing 100084, China

Abstract: In this paper, we report on the design, simulation and testing of a novel CZT detector with an electrode named the Strengthened Electric Field Line Anode (SEFLA). The Strengthened Electric Field (SEF) technique and Single Polarity Charge Sensing (SPCS) technique are implemented. It could achieve the same performance as Coplanar Grid, Pixel Array CZT detectors but requires only a simple readout system. Geant4, Ansoft Maxwell and a self-developed Induced Current Calculator (ICC) package are used to develop an understanding of how the energy spectrum is formed, and the parameters of the detector are optimized. A prototype is fabricated. Experimental results demonstrate the effectiveness of this design. The test shows that the SEFLA detector achieves a FWHM of 6.0% @59.5 keV and 1.6% @662 keV, which matches well with the simulations.

Key words: CZT detector, SEF technique, SPCS technique, gamma-ray spectroscopy

PACS: 29.30.Kv, 29.40.Wk **DOI:** 10.1088/1674-1137/38/12/126003

1 Introduction

The CZT detector has attracted much interest as a room-temperature semiconductor X-ray and gamma-ray detector (RTSD). Compared with Silicon and Germanium detectors, CZT detector operates at room temperature and has a higher stopping power due to the high density and high effective atomic number. Without the cooling system, the CZT detector can be made very compact and easy to operate. However, due to the severe hole trapping, spectroscopic performance is severely limited by the poor collection of holes for the thick conventional planar CZT detector. Many different electrodes implementing the single polarity charge sensing technique are proposed to improve the performance, like Frisch Grid, Coplanar Grid, CAPture^{TM} Plus, Pixel Array [1] Binode [2]. At the same time, many correction methods were developed, like rise time discrimination and Bi-parametric depth of interaction correction. By these techniques, nowadays the CZT detector performs better than any commercially available scintillator detector.

However, the high performance CZT detectors such as the Visual Frisch Grid detector, Coplanar Grid detector and the 3D depth sensing position sensitive detector require complex readout electronics and computation to do the correction [3–5]. We have exerted effort to develop a novel CZT detector, which requires only a single readout channel and can achieve the target performance with low cost.

2 Detector design

The typical structure of a conventional line anode detector [6] is shown in Fig. 1(left). In order to implement the strengthened electric field (SEF) technique, side cathodes are segmented into strips. Fig. 1(right) shows the structure of a SEFLA detector. The upper surface of the crystal is manufactured as a line anode. The bottom surface of the crystal is manufactured as a conventional cathode. Two opposite side surfaces are manufactured as strip electrodes. The coordinate system used in the following section is also shown in Fig. 1.

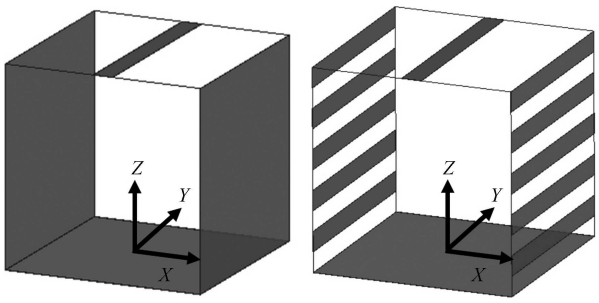

Fig. 1. (left)Line anode detector. (right) SEFLA detector.

Received 22 January 2014
∗ Supported by Ministry of Science and Technology of People's Republic of China (2011YQ040082)
1) E-mail: yulanli@mail.tsinghua.edu.cn
©2014 Chinese Physical Society and the Institute of High Energy Physics of the Chinese Academy of Sciences and the Institute of Modern Physics of the Chinese Academy of Sciences and IOP Publishing Ltd

Compared with the Coplanar Grid detector, the SEFLA detector has smaller capacitance and leakage current. SEFLA is suitable for large, cube crystal, while the Frisch Grid and CAPture^{TM} Plus are suitable for bar crystal and hemicube crystal, respectively.

In our work, the physical dimensions of the detector are fixed as 10 mm×10 mm×10 mm, which is now the commercial product. The design parameters of the SEFLA detector are the line anode width, the side strip pitch, the side strip gap, and the bias voltages applied on each electrode.

3 Simulation

3.1 Simulation process

Ansoft Maxwell is used to calculate the real electric field of CZT crystal and the weighting potential of the line anode. Export data is transferred as an input to the ICC package.

Geant4 [7] is used to simulate the initial interaction of gamma-ray in CZT crystal. The physics taken into account include the photoelectric effect, Compton scattering, pair production for gamma-rays and ionization for electrons. Energy deposition data is transferred as another input to the ICC package.

The ICC package is used to calculate a large set of numerical simulations aimed at understanding the influence of the design parameters and the forming of a spectrum. ICC is short for Induced Current Calculator, which is a self-developed C++ package. This package simulates the charge induction behavior of the device, and takes into account the properties of the CZT crystal, carriers transport in the electric field, carriers trapping and electronic noise.

Figure 2 gives a summarized schematic description of the simulation. The current induced on the anode by electrons and holes is calculated using the Shockley-Ramo theorem [8, 9]. Then the signal of the detector is convoluted with the readout of the electronics model. A large number of events are calculated and the spectrum is plotted.

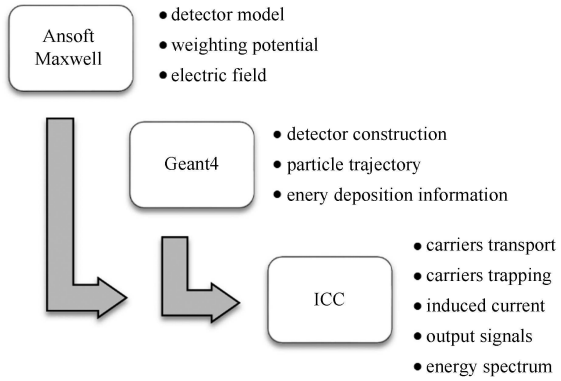

Fig. 2. Simulation process.

3.2 Crystal parameter

In reality, CZT crystal contains impurities and is not uniform; however, in our model, it is assumed that CZT crystal is uniform. We concentrate our attention on the behavior of carriers transport and trapping, because it determines the performance of the detector [10].

It is clearly established that the mobility-lifetime products of electron and hole are the first order dominant parameters influencing the performance of the detector, so is the bias voltage. The mobility-lifetime products used in the simulation are given in Table 1.

Table 1. CZT crystal parameters.

parameter	electrons	holes
mobility/($cm^2 \cdot V^{-1} \cdot s^{-1}$)	1000	50
lifetime/s	7E-6	1E-6
mobility×lifetime/($cm^2 \cdot V^{-1}$)	7E-3	5E-5
ionization potential/(eV/pair)	4.64	
Fano factor	0.089	

3.3 Electric field and weighting potential

The electric field and weighting potential of planar, line anode and SEFLA detectors are calculated by Ansoft Maxwell. Fig. 3 shows the comparison of the real potential and the weighting potential in the XZ plane (coordinate system is shown in Fig. 1). All these three structures are applied in the 1000 V bias.

The weighting potential of a planar anode is shown in Fig. 3(d). It is a linear distribution. According to the Shockley-Ramo theorem, holes will contribute a significant part to the induced charge in a planar detector. Due to the severe hole trapping, the spectroscopic performance of the planar CZT detector is severely limited.

Figure 3(e) shows the weighting potential of a line anode detector within the XZ plane. The weighting potential is greatly suppressed compared with that of a planar detector. Therefore, the induced charge of a line anode detector is dominated by the movement of electrons near the anode and the contribution of holes is eliminated. The single polarity charge sensing technique is implemented.

However, in the line anode detector, the real electric field near the bottom cathode is very weak, which is shown in Fig. 3(b). Carriers take a lot of time to transport from cathode to anode and are trapped a lot. SEFLA can overcome this problem. A bias voltage between anode and cathode is applied, and by applying increasing potentials on side strip electrodes from cathode to anode, the real electric field is strengthened. Fig. 3(c) shows the real electric potential of a SEFLA detector. It is clear that the electric field intensity is stronger in most regions compared with that of a line anode detector. The strengthened electric field (SEF) technique is implemented.

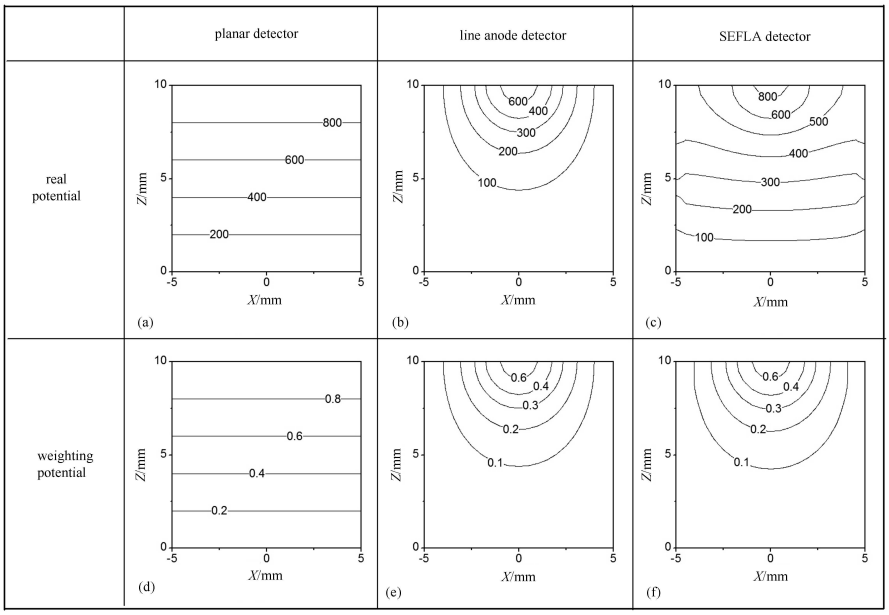

Fig. 3. Comparison of real potential and weighting potential. (a) Real potential of a planar detector; (b) real potential of a line anode detector; (c) real potential of a SEFLA detector; (d) weighting potential of a planar detector; (e) weighting potential of a line anode detector; (f) weighting potential of a SEFLA detector.

While the weighting potential of a SEFLA detector is nearly the same as that of a line anode detector, the SEFLA detector takes both advantages of the single polarity charge sensing (SPCS) technique and the strengthened electric field (SEF) technique.

3.4 Induced charge map

The idea of the basic structure of the SEFLA CZT detector is developed theoretically. The parameters of the detector need to be optimized. A large set of simulated data is generated by the ICC package, one selected result is presented to understand the influence of each parameter and to explain how the spectrum is formed.

The same energy deposited in different positions contributes different induced charge due to the carriers trapping. This phenomenon results in a poor spectral response. In order to find out the details, interactions within the XZ plane are studied. The same energy is deposited in different positions, and the induced charge corresponding to the position is calculated. Fig. 4 illustrates the induced charge map of one optimized design within the XZ plane.

The ideal charge induction map would be uniform if there was no trapping, and an excellent spectrum could be obtained. Considering trapping, the induced charge map shown in Fig. 4 indicates a fairly uniform response in the region far away from the anode and side strips. The region is circled out where the charge induction efficiency is larger than 95% (the maximum efficiency is normalized to 100% here). This region of the detector volume is the peak-forming region. While the interactions near the anode and side strips with small charge induction efficiency contribute to the low energy tail. This region of the detector volume is the low-tail region.

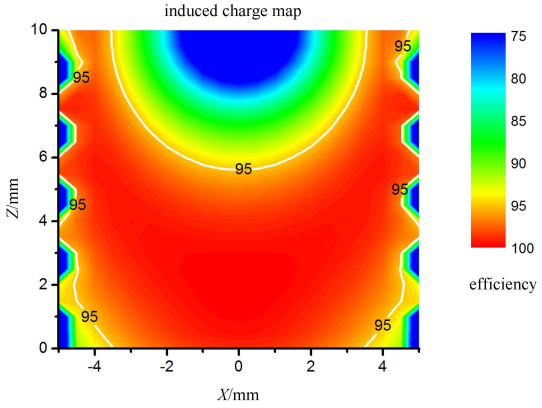

Fig. 4. Induced charge map within the XZ plane.

The reason for the low charge induction efficiency in the low-tail region is investigated. Simulation shows that charge sharing is the main reason for the interactions near the side strips while the severe hole trapping is the main reason for the interactions near the anode.

Smaller strip size and gap, smaller anode size are preferred to reduce the volume of the low-tail region. Higher bias voltage makes the carriers drift time shorter, which results in less trapping and reducing the low-tail region.

3.5 Simulated spectrum

Though a small strip size is preferred, it is difficult to fabricate. There is a tradeoff between cost and perfor-

mance. Finally, the number of side strips is set to five in the first prototype design. The parameter details are presented in the next section. The following part presents the simulated spectrum of the prototype. A Gamma source is inputted on the cathode side. 59.5 keV and 662 keV gamma-rays are simulated to study the detector's response. Electronic noise is assumed to be 4.0 keV (FWHM). The spectrums are plotted in Fig. 5.

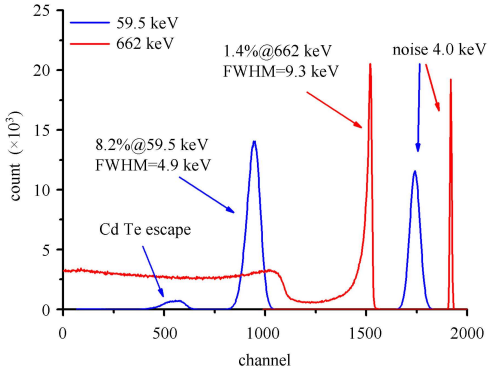

Fig. 5. Simulated spectrum.

Due to the high stopping power, most of the 59.5 keV gamma-rays interact within the 1 mm region near the cathode, which is located in the peak-forming region (Fig. 4). So no evident low energy tail is observed. Cd and Te X-rays escape peaks can be observed clearly. While high energy gamma-rays (662 keV) interact throughout the whole detector, a lot of gamma-rays interact in the low-tail region. So evident low energy tail is observed.

4 Experiment

4.1 Experiment setup

A Redlen CZT crystal is fabricated to study experimentally the SEF technique. The detector is 10 mm× 10 mm×10 mm. The width of the line anode is 1 mm. There are five side strip electrodes. The width of side strips is 1 mm, so is the gap between the side strips.

The first SEFLA CZT prototype is fabricated by Nuctech Company Limited and tested in Tsinghua University. Table 2 shows the voltages of each electrode when the bias voltage is 1000 V. The potentials applied on the side strip electrodes are changed proportionally when the bias voltage is changed.

4.2 Spectral response

The room-temperature responses of the prototype to ^{241}Am and ^{137}Cs are measured. Gamma-ray is irradiated from the cathode side. Measurements are taken under 1400 V bias and 0.5 μs shaping time. A thin copper slice is used to shield the 17 keV X-ray from ^{241}Am.

Table 2. Applied voltages.

electrode	bias voltage/V
anode	0
side strip 5	−520
side strip 4	−590
side strip 3	−700
side strip 2	−810
side strip 1	−940
cathode	−1000

The 59.5 keV spectrum is plotted in Fig. 6. The low energy tail at the full-energy peak of 59.5 keV is not evident. The peaks between the 100 and 200 channel are the escape peaks due to Cd and Te X-rays. Test pulse shows the electronic noise is about 3.4 keV (FWHM), which is very close to the detector resolution 3.6 keV @59.5 keV. The resolution @59.5 keV is mainly limited by the electronic noise, and the region near the cathode has a very good response.

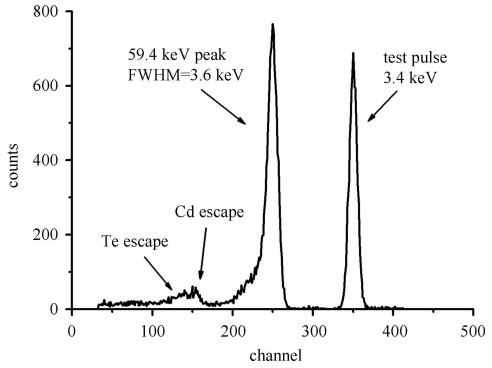

Fig. 6. Measured 59.5keV gamma-ray spectrum.

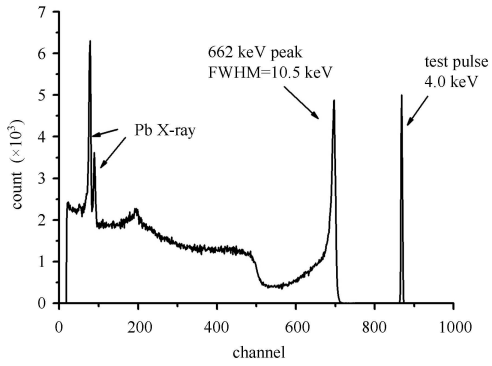

Fig. 7. Measured 662 keV gamma-ray spectrum.

A thin lead slice is used to shield the 32 keV X-ray from ^{137}Cs. The 662 keV spectrum is plotted in Fig. 7. The Pb X-ray peaks are evident and separated well. The low energy tail at the full-energy peak of 662 keV is very evident. The test pulse shows the electronic noise is about 4.0 keV (FWHM), which is much smaller than the detector resolution 10.5 keV @662 keV. The resolution @662 keV is mainly limited by the whole detector response.

4.3 Response linearity

Detector linearity is one of the most important specifications for a detector.The linear fit plotted in Fig. 8 indicates that the prototype response linearity is very good. An R-square is nearly equal to 1.

Five peaks are used to do the linear fit, shown in Table 3.

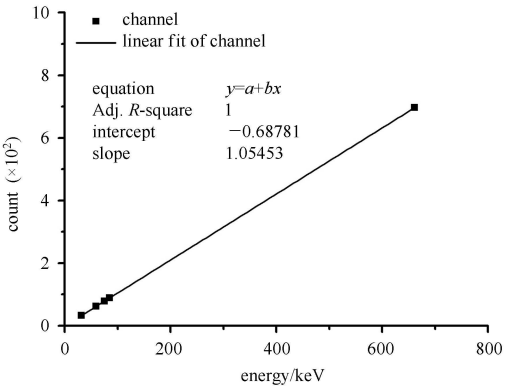

Fig. 8. Detector energy response linearity.

Table 3. Peaks used to fit.

source	energy/keV	channel number
^{137}Cs	661.6	697
Pb X-ray	84.90	89
Pb X-ray	74.97	78
^{241}Am	59.5	62
^{137m}Ba X-ray	31.80	33

4.4 Bias dependence

The mobility-lifetime products and the bias voltage are both the first order dominant parameters influencing the performance of a detector, as mobility-lifetime products are determined by the crystal itself, but the bias voltage can be changed to improve the detector performance. Spectrums are measured under different bias voltages.

Figure 9 gives the resolution-bias voltage curve. The resolution becomes better while bias voltage increases from 900 V to 1400 V. When the bias voltage is high enough, the resolution is improved very little because of the increasing leakage current.

With higher bias voltage, the electric field is stronger. The drift time of carriers will be shorter so electrons trapping decreases, and more electrons can be collected by the anode. So the output signal is bigger and the full-energy peak channel number becomes bigger. The curve plotted in Fig. 9 is not saturated under 1400 V bias. Higher bias voltage is preferred to improve the resolution if the leakage current increasing is not significant. Efforts will be made to reduce the leakage current by a better surface treatment process.

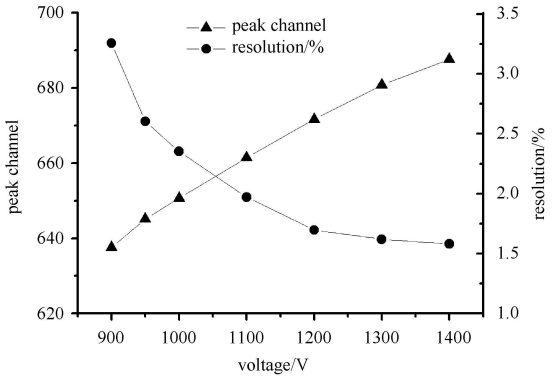

Fig. 9. Resolution/Peak channel-Bias curve.

5 Summary

In this study, we have designed a SEFLA detector by implementing a single polarity charge sensing (SPCS) technique and strengthened electric field (SEF) technique. A self-developed ICC package is used to study the dependence of the performance on the design parameters and to optimize its parameters. The induced charge map is plotted to understand how the spectrum is formed.

One prototype is fabricated, tested, and demonstrates a good performance. Measurement results match well with the simulations, which verifies that our design and ICC package are correct. The FWHM of this prototype is 6.0% @59.5 keV and 1.6% @662 keV without any correction. Better resolution can be achieved by using lower noise electronics and depth of interaction correction.

References

1 HE Z. Nucl. Instrum. Methods A, 2001, **463**(1): 250–267
2 NIU L B, LI Y L et al. Nuclear Science and Techniques, 2014, **25**: 010406
3 Bolotnikov A E, Abdul-Jabbar N M, Babalola S et al. Optical Engineering Applications. International Society for Optics and Photonics, 2007. 670603-670603-14
4 Luke P N. IEEE Trans. Nucl. Sci., 1995, **42**(4): 207–213
5 HE Z, LI W, Knoll G F et al. Nucl. Instrum. Methods A, 1999, **422**: 173–178
6 ZHANG L, LI Y L, LI Y J et al. Performance improvement of CZT detectors by line electrode geometry. Greece, The 2013 International Conference on Applications of Nuclear Techniques. 2013
7 Agostinelli S, Allison J, Amako K et al. Nucl. Instrum. Methods A, 2003, **506**(3): 250–303
8 Shockley W. J. Appl. Phys., 1938, **9**: 635–636
9 Ramo S. Proceedings of the IRE, 1939, **27**(9): 584–585
10 Bale D S, Szeles C. Optics & Photonics. International Society for Optics and Photonics, 2006. 63190B-63190B-11